J Supercond Nov Magn (2016) 29:2729–2734
DOI 10.1007/s10948-016-3792-8

REVIEW PAPER

Studies on the Properties of Manganese Substituted Nickel Ferrite Nanoparticles

R. Kesavamoorthi[1] · C. Ramachandra Raja[1]

Received: 12 May 2016 / Accepted: 13 August 2016 / Published online: 14 September 2016

Abstract Mn^{2+}-substituted Ni ferrite nanoparticles were synthesized by sol-gel auto combustion method. The synthesized samples were annealed at 800 °C and characterization studies were carried out by XRD, VSM, electron paramagnetic resonance (EPR), field emission scanning electron microscopy (FE-SEM) and FT-IR spectroscopy. The XRD patterns revealed that Mn^{2+}-substituted Ni ferrite crystallizes in cubic spinel phase and addition of α-Fe_2O_3 phase was also observed. The average crystallite sizes were found to be from 42 to 56 nm using a Scherer equation. The coercivity and remanent magnetization decreases when Mn^{2+} ion concentration is increased. The EPR spectrum shows the phase homogeneity of the samples. The FE-SEM images revealed that particles are both spherical in shape and particle sizes varied from 22 to 41 nm. The FT-IR spectrum confirmed the two main metal ion vibrations of nickel ferrite near 550 to 560 cm^{-1} (A site) and 441 to 460 cm^{-1} (B site).

Keywords Mn-Ni ferrite · Sol-gel combustion · Structural · Magnetic properties

1 Introduction

Spinel ferrites are extensively used for technological applications because of their special electrical and magnetic properties. Spinel ferrite compounds are used in the production of electronic sensors, memory devices, carriers of drug, magnetic resonance imaging devices and multilayer chip inductors [1, 2]. The magnetic properties of these ferrites can be changed by the substitutions of various kinds of metal ions (Mn^{2+}) among divalent cations or by introducing a relatively small amount of rare-earth ions [3, 4]. The structural formula of ferrite is $A^{2+}B_2^{3+}O_4$, where A is a divalent metal ion (Ni^{2+}, Zn^{2+}, Mn^{2+}, etc.) and B is a trivalent metal ion (Fe^{3+}, Al^{3+}, Sr^{3+}, etc.) [5]. The properties of the ferrites can be tuned by varying the cation substitution and their distribution among tetrahedral site and octahedral site. In Mn^{2+}-substituted $NiFe_2O_4$, the Ni^{2+} ions occupy octahedral (B) sites and Mn^{2+} ions occupy tetrahedral (A) and octahedral (B) sites. Ferrites containing Mn^{2+} ions have a tendency to form α-Fe_2O_3 phase when heat treated above 200 °C in air atmosphere [6]. The properties of ferrites are dependent on their structural parameters of particle size and shape, which can be modified in the synthesis processes. In spinel ferrites, the structural and magnetic properties are strongly dependent on cation distribution and method of preparation [7, 8]. Synthesis of ferrite materials includes co-precipitation method, solvothermal technique, ball milling method, hydrothermal processing, sol-gel method, etc. [9–13]. Among all the methods, the sol-gel combustion method is widely used for the synthesis of ferrite due to its advantages of preparation, composition flexibility, homogeneity, and low cost.

In the present work, the results obtained in the studies on $Mn_xNi_{1-x}Fe_2O_4$ ($x = 0, 0.2, 0.4, 0.6$) ferrite nanoparticles annealed at 800 °C are reported. Powder X-ray diffraction (XRD), vibrating sample magnetometer (VSM), electron paramagnetic resonance (EPR), field emission scanning electron microscopy (FE-SEM) and FT-IR spectroscopy techniques were employed for structural and magnetic characterizations. The structural and magnetic properties are discussed and compared with earlier reports.

✉ C. Ramachandra Raja
crraja_phy@yahoo.com; crrajaphy@gmail.com

[1] Department of Physics, Government Arts College (Autonomous), Kumbakonam 612 002, India

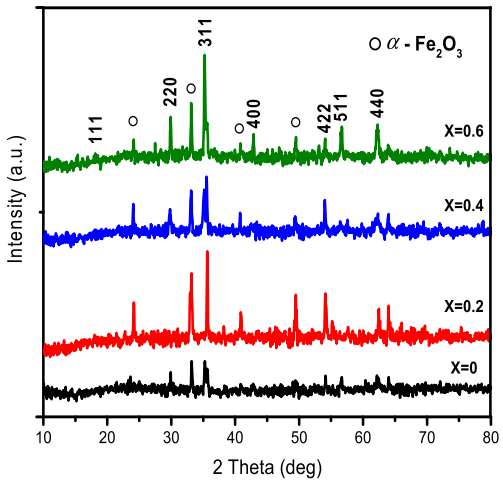

Fig. 1 XRD patterns of the $Mn_xNi_{1-x}Fe_2O_4$ samples ($x = 0, 0.2, 0.4, 0.6$)

2 Material and Methods

2.1 Synthesis of Mn^{2+}-Substituted Ni Ferrite Nanoparticles

Mn^{2+}-substituted Ni ferrites of chemical composition $Mn_xNi_{1-x}Fe_2O_4$ samples ($x = 0$, 0.2, 0.4, 0.6) were synthesized by a sol-gel combustion method at room temperature using analytical reagent grade iron nitrate $Fe(NO_3)_3.9H_2O$, nickel nitrate ($Ni(NO_3)_2.6H_2O$), manganese nitrate ($Mn(NO_3)_2.6H_2O$), tartaric acid and ammonia (NH_3) solution. An appropriate amount of each material in stoichiometric ratio was dissolved in de-ionized water. The mixed nitrate solution was heat treated at 60 °C the solution became dehydrated and then the gel formation took place. The gel was dried in the hot air oven at 120 °C for 8 h. The final powder was annealed at 800 °C using a muffle furnace at a heating rate of 5 °C/min. The structural and phase analyses of synthesized samples were done by XRD technique using an X'Pert Pro Pan analytical X-ray diffractometer operated at 45 kV and 30 mA, Cu Kα, wavelength 1.5406 Å. Room-temperature magnetization studies were performed using a VSM (Lake Shore model 7404) operated at a field of 15 kOe. The g value and peak-to-peak line width (ΔH_{pp}) of the samples were calculated at room temperature using a Bruker BioSpin EMX Plus EPR spectrometer operated at 100 kHz modulation frequency and 9.86 GHz microwave frequency. The morphology and particle size measurements were characterized by FE-SEM (model JEOL/JSM 6701F). FT-IR spectra were recorded by a Perkin Elmer FT-IR spectrometer using KBr pellets, in the range of 4000–400 cm^{-1}.

3 Results and Discussion

3.1 Structure and Phase Analysis of Mn^{2+}-Substituted Ni Ferrite Nanoparticles

The XRD patterns of Mn substituted Ni ferrite samples are shown in Fig. 1. The XRD pattern revealed that all the diffracted peaks are related to cubic spinel phase and the addition of small peaks as secondary phase (α-Fe_2O_3) is also observed in the Mn^{2+}-substituted Ni ferrite samples. The prominent (*hkl*) planes (111), (220), (311), (400), (422), (511), and (440) are indexed in the pattern. The intensity of these peaks increases with an increase in the concentration of Mn^{2+} ion. The XRD patterns of Mn-Ni ferrite samples match with the Joint Committee of Powder Diffraction Standards (JCPDS) (Card No.: 75-0894) and all the experimental XRD planes perfectly match with earlier reported studies [14].

The average crystallite size has been calculated using the Scherer equation

$$D = \frac{0.9\lambda}{\beta \cos\theta}$$

where D is the average crystallite size, λ is the wavelength of the X-ray radiation used ($\lambda = 1.5406$ Å), β denotes the full width at half maximum (FWHM) measured in radians and θ is the Bragg angle [15]. The average crystallite size of synthesized samples is found to be from 42.4 to 56.7 nm. The crystallite size is slightly increased with an increasing level of Mn^{2+} concentration. The lattice constant (a) of synthesized ferrite samples was calculated by using the Bragg equation

$$d = \frac{a}{\sqrt{h^2 + k^2 + l^2}}$$

Table 1 Structural properties of the Mn substituted Ni ferrite samples

Samples (x)	Lattice constant (a) (Å)	Volume (Å^3)	X-ray density (g/cm^3)	Crystallite size	
				XRD (nm)	FE-SEM (nm)
$NiFe_2O_4$	8.355	603	5.255	42.47	22–30
$Mn_{0.2}Ni_{0.8}Fe_2O_4$	8.473	600	5.069	42.48	22–32
$Mn_{0.4}Ni_{0.6}Fe_2O_4$	8.439	608	5.169	42.49	23–33
$Mn_{0.6}Ni_{0.4}Fe_2O_4$	8.451	583	5.193	56.71	22–41

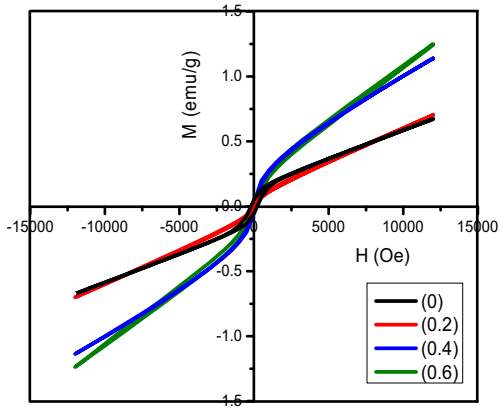

Fig. 2 M–H plots of the $Mn_xNi_{1-x}Fe_2O_4$ samples ($x = 0$, 0.2, 0.4, 0.6)

where d is the inter-planar distance and h, k, and l are the Miller indices. The lattice constant values of synthesized Mn^{2+}-substituted Ni ferrite samples are presented in Table 1. The present results indicate that Mn^{2+}-substituted Ni ferrite samples have slightly higher lattice constant values. This may be due to the replacement of smaller ionic radius Ni^{2+} (0.69 Å) ion by larger ionic radius Mn^{2+} (0.83 Å) ion. This causes the lattice expansion. The X-ray density (ρ_x) was calculated using the equation

$$\rho_x = \frac{8M}{Na^3}$$

where 8 represents the number of atoms in a unit cell of spinel lattice, M is the molecular weight of the Mn substituted Ni ferrite samples, N is Avogadro's number (6.02252×10^{26} $kmol^{-1}$) and a is the lattice constant. The X-ray densities of the synthesized samples are found to be from 5.19 to 5.25 g/cm^3. The X-ray density values were found to decrease with an increase in Mn^{2+} concentration. All structural parameters of Mn^{2+}-substituted Ni ferrite samples are calculated and listed in Table 1. The results are in good agreement with the result reported by Tirupanyam et al. [16] and Hassan et al. [17].

Table 2 Magnetic properties of the Mn-substituted Ni ferrite samples

Composition (X)	Samples (X)	H_c (Oe)	M_r (emu/g)
0	$NiFe_2O_4$	200	0.100
0.2	$Mn_{0.2}Ni_{0.8}Fe_2O_4$	110	0.075
0.4	$Mn_{0.4}Ni_{0.6}Fe_2O_4$	70	0.050
0.6	$Mn_{0.6}Ni_{0.4}Fe_2O_4$	60	0.025

3.2 VSM Analysis of Mn^{2+}-Substituted Ni Ferrite Nanoparticles

Analysis of the magnetic behavior of the Mn_xNi_{1-x} ferrite samples was carried out using a vibrating sample magnetometer. Variation of magnetization (M, emu/g) with the applied field (H, Oe) at room temperature is shown in Figs. 2 and 3. The magnetic properties such as coercivity (H_c) and remanent magnetization (M_r) values are measured from the plotted hysteresis (M–H) loops and are listed in Table 2. At room temperature, the very narrow loops for all the samples indicate the soft magnetic nature [18, 19]. Non-saturation of magnetization even at an applied field of 12.5 kOe reveals the presence of single-domain nanoparticles in superparamagnetic state. The coercivity of Ni ferrite is 200 Oe. The addition of Mn^{2+} ions decreases the coercivity. The decrease of H_c is due to the decrease of Ni^{2+} content. The slight changes in coercivity due to an increase of Mn^{2+} ions may be attributed to domain structure, critical diameter, lattice strain, and shape anisotropy of crystal. The results are in good agreement with the results reported in the literature [20–23].

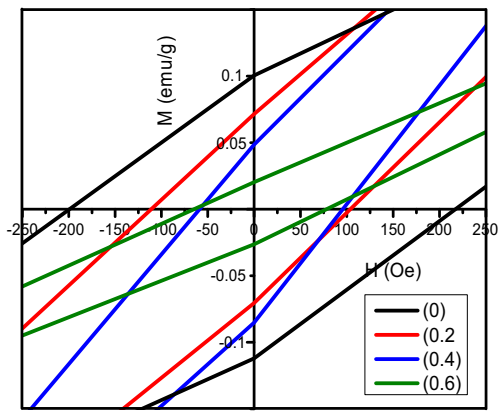

Fig. 3 M–H enlarged plots of the $Mn_xNi_{1-x}Fe_2O_4$ samples ($x = 0$, 0.2, 0.4, 0.6)

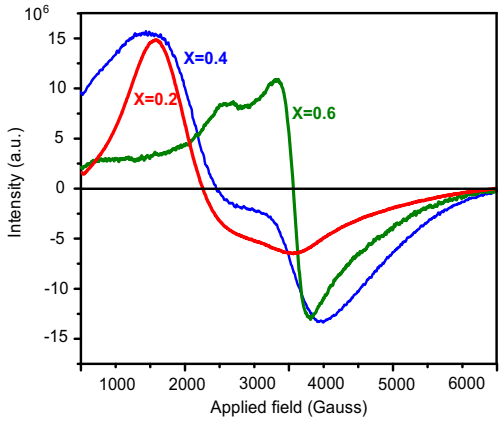

Fig. 4 EPR spectra of the $Mn_xNi_{1-x}Fe_2O_4$ samples ($x = 0.2$, 0.4, 0.6)

Table 3 EPR parameters of the Mn substituted Ni ferrite samples

Composition (X)	Samples	Resonance field, H_r (G)	g value	Line width, ΔH_{pp} (G)
0.2	$Mn_{0.2}Ni_{0.8}Fe_2O_4$	2250	3.131	1950
0.4	$Mn_{0.4}Ni_{0.6}Fe_2O_4$	2500	2.817	2500
0.6	$Mn_{0.6}Ni_{0.4}Fe_2O_4$	3050	2.012	500

3.3 EPR Spectra Analysis

Powder EPR spectral measurement is an essential investigation for the magnetic materials because at high frequencies the resonance occurs due to the interaction between electron spin and electromagnetic waves. The EPR spectra of synthesized Mn^{2+}-substituted Ni ferrite samples were recorded at room temperature and are shown in Fig. 4. For all the samples, the obtained spectra show single and broad resonance peaks. This reveals that isolated Fe^{3+}, Ni^{2+}, and Mn^{2+} ions do not exist and also reveals the phase homogeneity of the prepared samples [24]. The spectrum was analyzed to obtain values of the magnetic field at resonance position corresponding to zero signals (H_r), peak-to-peak line width (ΔH_{pp}), and effective g value. The obtained values are presented in Table 3.

The g value was calculated using

$$g = \frac{h\upsilon}{\beta H_r}$$

where h is Planck's constant (6.6234×10^{-34} Js), υ is the microwave frequency (9.86 GHz), β is the Bohr magneton (9.274×10^{-24} Am^2) and H_r is the magnetic field at resonance. The observed values of resonance field (H_r) and g factor are in general dependent on the magnetic dipole interactions among nanoparticles and the super-exchange interaction between Ni^{2+}, Mn^{2+}, and Fe^{3+} ions through nonmagnetic O^{2-} ions [25, 26].

3.4 FE-SEM Analysis of Mn^{2+}-Substituted Ni Ferrite Nanoparticles

Figure 5 shows the FE-SEM micrographs of synthesized $Mn_xNi_{1-x}Fe_2O_4$ nanoparticles. As seen from FE-SEM images, the samples consist of mostly spherical-shaped particles. FE-SEM images show that there is development of grain structure with annealing temperature.

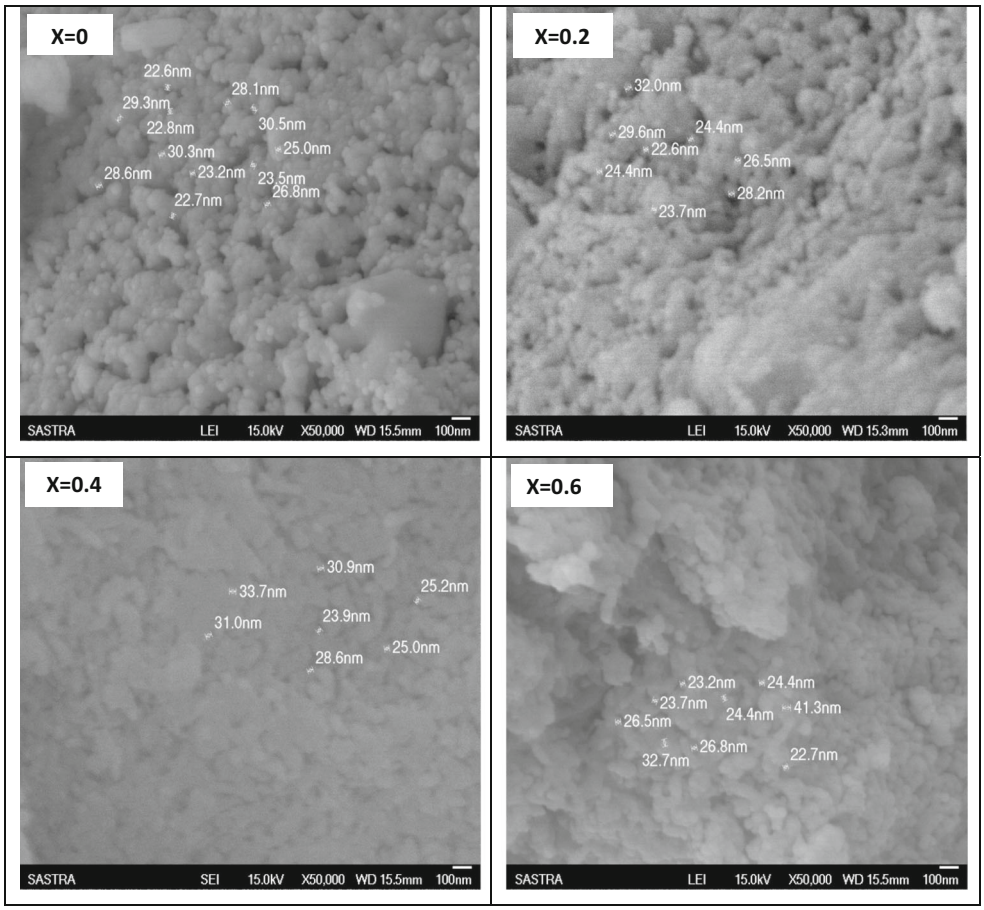

Fig. 5 FE-SEM images of the $Mn_xNi_{1-x}Fe_2O_4$ samples ($x = 0, 0.2, 0.4, 0.6$)

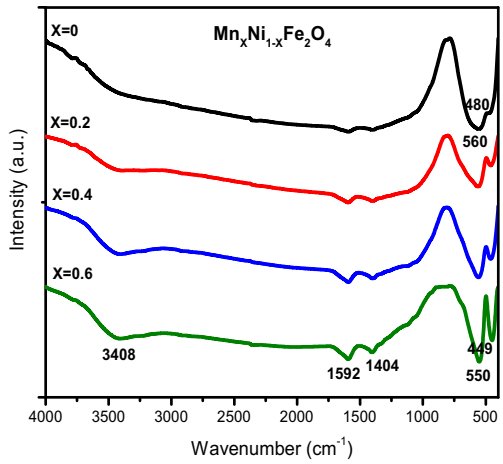

Fig. 6 FT-IR spectrum of the $Mn_xNi_{1-x}Fe_2O_4$ samples ($x = 0$, 0.2, 0.4, 0.6)

Mn^{2+}-substituted Ni ferrite synthesized and annealed at 800 °C composed of agglomerated spherical particles.

Increasing the Mn^{2+} ion concentration, the powders show irregular microstructures with small spherical particles and size of the particle ranging from 22 to 41 nm [27]. Generally, the grain size increases with an increase in Mn^{2+} ion concentration. The particles are spherical in shape, and the size and structural morphology of the particles varied in different levels of Mn compositions.

3.5 FT-IR Spectroscopy Analysis

The FT-IR spectra of synthesized Mn substituted Ni ferrite samples are shown in Fig. 6. The FT-IR spectra revealed that the region of the spectrum, centered around at 3411 and 3408 cm^{-1} represents the stretching vibration of a hydroxyl group of water molecules (–OH) present in the samples. The frequencies around 1592 and 1405 cm^{-1} are assignable as a metal ferrite (M/Fe) complex present in the samples.

The two main metal-oxygen vibrations are observed at 550 to 560 cm^{-1} and at 449 to 480 cm^{-1} due to tetrahedral and octahedral sites, respectively. The band near 550 to 560 cm^{-1} corresponds to an intrinsic stretching vibration of metal of the tetrahedral site (metal oxide), whereas the bands at 449 to 480 cm^{-1} are assigned to octahedral sites (Fe–O). The results are in good agreement with the result reported by Koseoglu et al. [28].

4 Conclusion

Manganese substituted nickel ferrite nanoparticles were synthesized at room temperature by a sol-gel auto combustion method. The XRD pattern revealed that the Mn substituted Ni ferrite has a cubic spinel structure. The VSM analysis revealed that the Mn substituted Ni ferrite nanoparticles were in superparamagnetic state at room temperature. The coercivity and remanent magnetization values were found to be decreased. The g value decreases with an increase in Mn^{2+} ion concentration. The surface morphology of the ferrite samples is spherically shaped and size of the ferrites was found to be from 22 to 41 nm. The FT-IR spectrum confirmed that two main metal ion vibrations are observed in the spectrum. It is concluded that substituted manganese ion strongly affects the magnetic and structural properties of nickel ferrite.

Acknowledgments The authors gratefully acknowledge the financial support provided by the Tamilnadu State Council for Science and Technology (TNSCST), Chennai (TNSCST/S&T Projects/PS/RJ/2013-2014). The authors would also like to thank the Pondicherry University, Puducherry, India, for the VSM characterization facilities; the St. Joseph's College, Trichy, for the FT-IR spectra; the SASTRA University, Thanjavur, for the FE-SEM facilities; and the Alagappa University, Karaikudi, for the powder XRD facilities.

References

1. Camley, R.E., Celinski, Z., Fal, T., Glushchenko, A.V., Hutchison, A.J., Khivintsev, Y., Harward Bijoy Kuanr, I.R., Veerakumar, V.: High-frequency signal processing using magnetic layered structures. J. Magn. Magn. Mat. **321**, 2048–2054 (2009)
2. Koseoglu, Y., Alan, F., Tan, M., Yilgin, R., Ozturk, M.: Low temperature hydrothermal synthesis and characterization of Mn doped cobalt ferrite nanoparticles. Ceram. Int. **38**, 3625–3634 (2012)
3. Snelling, E.C.: Soft ferrites, Properties and Applications. 2nd edn., p. 36. Butter Worth and Co. (Publisher) Ltd, London (1988)
4. Yang, Y.B., Liu, S.Q., Zhao, H., Yang, W.Y., Wu, R., Huang, Q.Z., Zhou, D., Du, H.L., Wang, C.S., Yang, Y.C., Xu, H., Zhu, J.L., Gourdon, O., Vogel, S., Yang, J.B.: Magnetic structure and phase transition of $Ni_2Mn_{1.48}Sb_{0.52}$ magnetic shape memory compound. Scripta Materialia **116**, 31–35 (2016)
5. Sutka, A., Mezinskis, G., Lusis, A., Jakovlevs, D.: Influence of iron non-stoichiometric on spinel zinc ferrite gas sensing properties. Sensors Actuat. B **171**, 204–209 (2012)
6. Sharifi, I., Shokrollahi, H., Amiri, S.: Ferrite-based magnetic nanofluids used in hyperthermia applications. Magn. Magn. Mat. **324**, 903–915 (2012)
7. Maaz, K., Karim, S., Mumtaz, A., Hasanain, S.K., Liu, J., Duan, J.L.: Synthesis and magnetic characterization of nickel ferrite nanoparticles prepared by co-precipitation route. Magn. Magn. Mat. **321**, 1838–1842 (2009)
8. Hui, D.C., Xue, W.G., Lei, S., Wei, G.D., Jun, J.C., Sheng, X.D.: Investigation of the thermal stability of Mn ferrite particles synthesized by a modified co-precipitation method. Sci. China Phys. Mech. Astron. **56**(3), 568–572 (2013)
9. Ashiqa, M.N., Saleema, S., Malana, M.A., Anis-Ur-Rehman: Physical, electrical and magnetic properties of nanocrystalline Zr-Ni doped Mn-ferrite synthesized by the co-precipitation method. J. Alloys Compd. **486**, 640–644 (2009)
10. Aslibeiki, B., Kameli, P., Ehsani, M.H., Salamati, H., Muscas, G., Agostinelli, E., Foglietti, V., Casciardi, S., Peddis, D.: Solvothermal synthesis of $MnFe_2O_4$ nanoparticles: the role of polymer coating on morphology and magnetic properties. Magn. Magn. Mat. **399**, 236–244 (2016)

11. Hajalilou, A., Hashim, M., Ebrahimi-Kahrizsangi, R., Kamari, H.M.: Influence of evolving microstructure on electrical and magnetic characteristics in mechanically synthesized polycrystalline Ni-ferrite nanoparticles. J. Alloys Compd. **633**, 306–316 (2015)
12. Chae, K.P., Choi, W.O., Kang, B.-S., Choi, S.H.: Crystallographic and magnetic properties of nickel substituted manganese ferrites synthesized by sol-gel method. J. Magn. **18**(1), 21–25 (2013)
13. Hessien, M.M., Zaki, Z., Mohsen, A.-Q.: Low-temperature synthesis of nanocrystalline $Mn_{0.2}Ni_{0.8}Fe_2O_4$ by oxalate precursor route. Adv. Mater. Phys. Chem. **3**, 1–7 (2013)
14. Ranjithkumar, E., Jayaprakash, R., Seehra, M.S., Prakash, T., Kumar, S.: Effect of a-Fe_2O_3 phase on structural, magnetic and dielectric properties of Mn-Zn ferrite nanoparticles. Phys. Chem. Solids **74**, 943–949 (2013)
15. Cullity, B.D.: Elements of X-ray Diffraction. 2nd edn., p. 89. Addison-Wesley, London (1978)
16. Tirupanyam, B.V., Srinivas, C., Meena, S.S., Yusuf, S.M., Satish Kumar, A., Sastry, D.L., Seshubai, V.: Investigation of structural and magnetic properties of co-precipitated Mn-Ni ferrite nanoparticles in the presence of α-Fe_2O_3 phase. Magn. Magn. Mat. **392**, 101–106 (2015)
17. Hassan, H.E., Sharshar, T., Hessien, M.M., Hemed, O.M.: Effect of c-rays irradiation on Mn-Ni ferrites: structure, magnetic properties and positron annihilation studies. Nuclear Inst. Methods Phys. Res. B **304**, 72–79 (2013)
18. Nejati, K., Zabihi, R.: Preparation and magnetic properties of nano size nickel ferrite particles using hydrothermal method. Chem. Central **23**, 1–6 (2012)
19. Airimioaei, M., Ciomaga, C.E., Apostolescu, N., Leontie, L., Iordon, A.R., Mitoseriu, L., Palamaru, M.N.: Synthesis and functional properties of the $Ni_{1-x}Mn_xFe_2O_4$ ferrites. J. Alloys Compd. **509**, 8065–8072 (2011)
20. Shobana, M.K., Sankar, S.: Structural, thermal and magnetic properties of $Ni_{1-x}Mn_xFe_2O_4$ nanoferrites. Magn. Magn. Mat. **321**, 2125–2128 (2009)
21. Balaji, G., Gajbhiye, N.S., Wilde, G., Weissmuller, J.: Magnetic properties of $MnFe_2O_4$ nanoparticles. Magn. Magn. Mat. **242–245**, 617–620 (2002)
22. Koseoglu, Y., Bay, M., Tan, M., Baykal, A., Sozeri, H., Topkaya, R., Akdogan, N.: Magnetic and dielectric properties of $Mn_{0.2}Ni_{0.8}Fe_2O_4$ nanoparticles synthesized by PEG-assisted hydrothermal method. Nanopar. Res. **13**, 2235–2244 (2011)
23. Raju, K., Balaji, C.G., Venugopal Reddy, P.: Microwave properties of Al and Mn doped nickel ferrites at Ku band frequencies. Magn. Magn. Mat. **354**, 383–387 (2014)
24. Baykal, A., Kasapoglu, N., Koseoglu, Y., Topark, M.S., Bayrakdar, H.: CTAB-assisted hydrothermal synthesis of $NiFe_2O_4$ and its magnetic characterization. J. Alloys Compd. **464**, 514–518 (2008)
25. Shahane, G.S., Zipare, K.V., Pant, R.P.: Synthesis and characterization of superparamagnetic Fe_3O_4 nanoparticles for ferrofluid applications. J. Magnetohydrodyn. **49**(3–4), 317–321 (2013)
26. Chand, M., Kumar, A., Annveer, K.S., Shankar, A., Pant, R.P.: Investigations on the $Mn_XZn_{1-X}Fe_2O_4$ (X = 0.1, 0.3 and 0.5) nanoparticles synthesized by sol-gel and co-precipitation methods. Ind. J. Eng. Chem. Mate. Sci **4**(8), 14–17 (2011)
27. Ranjith Kumar, E., Siva Prasada Reddy, P., Sarala Devi, G., Sathiyaraj, S.: Structural, dielectric and gas sensing behavior of Mn substituted spinel MFe_2O_4 (M = Zn, Cu, Ni, and Co) ferrite nanoparticles. Magn. Magn. Mat. **398**, 281–288 (2016)
28. Koseoglu, Y.: Structural, magnetic, electrical and dielectric properties of $Mn_xNi_{1-x}Fe_2O_4$ spinel nano ferrites prepared by PEG assisted hydrothermal method. Ceram. Int. **39**, 4221–4230 (2013)